THE EFFECT OF GLAZE ICING ON WING AERODYNAMICS AND AIRCRAFT LATERAL STABILITY

G. G. NAIR

A. Q. CHAPLEO

Department of Aeronautical Engineering
The Queen's University of Belfast
Belfast, Northern Ireland
United Kingdom.

ABSTRACT

The investigation was prompted by the crash of an aircraft where glaze - icing on the wing led to uncontrollable oscillations in roll. An aerodynamic model simulating the lateral stability and control characterestics of an iced wing is introduced. Experimental investigations and subsequent dynamic stall effects observed for a wing with leading edge ice is reported. Results establish the liability of glaze ice affecting the aircraft lateral stability and control characterestics which caused the accident.

INTRODUCTION

The experimental investigation was prompted by the crash of a **Shorts SD3 -60** aircraft where glaze icing on the wing caused uncontrolable oscillations in roll. (Fig. 1). Despite pilot corrective action, increasing roll oscillations encountered, peaking at c 55°, induced an increased rate of descent and sabsequent impact with the ground. Accident investigations[1] highlighted the meteorological conditions, the crew actions and flight tests on a Shorts SD3-60. Meteorological conditions which emphasised the presence of stratocumulus clouds indicated a strong possibility of airframe icing. Standard anti-icing and de-icing precautious taken by the crew were beyond criticism. Flight tests on a clean winged aircraft demonstrated

normal rates of roll damping. These facts isolated undetected ice accretion as the cause of the accident. The investigations concluded that undetected accretion of clear ice on the wing could have degraded the lateral stability and control characterestics of the aircraft. Accident Flight data is reproduced in Fig. 2.

ICE ACCRETION AND PROTECTION

The principal cause of atmospheric ice accretion are the supercooled water droplets present in clouds at sub Zero temperatures, which Freeze on impact with the airframe. For temperatures below -12°c, freezing occurs immediately on impingement forming the streamlined translucent rime ice. For temperatures greater than -12°c, the water droplets run up or down the stagnation point before freezing, forming the transparent double horned glaze ice. Glaze ice is transpatent and not visually detected at night easily. Ice profiles are illustrated in Fig. 3.

The employment of protection methods such as anti-icing and de-icing systems is a generally accepted procedure for controlling icing risk. However, accoring to standard precautions, de-icing devices such as the inflatable rubber boots in SD3-60 are not generally activated until ice has been visually detected. De-icing boots have strong limitations for severe icing conditions where it forms an air-tunnel between ice and leading edge of wing which is aerodynamically very unfavourable.

THE THEORETICAL MODELS

The validity of aerodynamic data obtained from the accident investigations was confirmed through preliminary simulation tests. Glaze ice again emerged as the strong possibility.

An intuitive model was suggested by Dr. A. Q. CHAPLEO. It stated that the twin horn geometry of glaze ice can cause double values of lift

coefficient in the aerofoil lift curve. The model predicted that flow separation from either horn might be introduce a hysteresis effect over a range of angles of attack. It was further argued that the flow encountered over a critical range of anlges of attack would depend to a greater extent on the direction of motion than on the frequency. In addition, lower values of lift curve slope compared to clean aerofoil were also expected. in Fig. 4.

Absence of stall warning was a particular point of concern which extended interest into the dynamic stalling characterestics of a glaze iced wing. The model, refered to as 'The stalled wing model', predicted a premature stall, based on flow separation caused by the twin horn geometry. Possible descrepencies in roll damping were forecast at stalling incidences in conjunction with the previous hysteresis model and rough strip theory estimates. The influence of direction of change of AOA at stalling incidences were expected to cause separation induced unsteady patterns.

FLIGHT TESTS AND COMPUTER SIMULATIONS

Flight tests performed[1] on a shorts SD3-60 with clean wing demonstrated normal responses to control inputs. Tests included variation of aileron and rudder inputs at constant frequency and eventual centralisation. Recovery was immediate even for high bank angles. The artificial stall warning system of SD3-60 was tested. Stall warning comprising stick shake and horn was indicated at 7 Kt IAS above the stalling speed. With power off, the warning was followed by a light airframe buffet and a rolling tendency controlable by aileron inputs. At stall, a remarkable descent rate was observed, but recovery was immediate upon release of rearward pressure on the control column. However, with icing trails, there were occasions with 2.75 inches thick glaze-ice where stall occured upto 20Kt IAS above stalling speed. Malfunctioning of leading edge stall warning devices were also observed. Test Flight data is graphically represented In Fig. 5.

Extensive simulation studies[2] using an interactive digital simulation package ISIS provided values for the roll damping and

aileron rolling moment derivatives, compared within the programme. The aileron inputs proved effective in simulating flights with clean wing but failed when the ice model was introduced. The theoretical hysteresis model was tested for the real control situation with a linear combination of roll rate, roll acceleration and bank angles. The accident was simulated using numerous icing models and control inputs. An interesting aspect of the results was a notable phase differece of 180° in aileron angle vs bank angle. This indicated that ailerons drove rather than controlled the roll oscillations. Simulations of lateral motion also indicated a high descent rate comparable with the accident aircraft.

WIND TUNNEL TESTING

Tests were conducted on a wing 0.45m chord, 0.836m span fitted with end plates in a low speed tunnel of section 0.835m x 1.14m. The model employed a Wortman FX67 K170 section having a maximum thickness of 17% at 40% chord. It includes 60% of chord laminar flow at test Reynolds number of 1.2×10^6 . Notable performance characterestics of the section include high lift coupled with low drag at low angles of attack and a smooth stall at high angles of attack. The SD 360 section employs a modified NACA 63 aerofoil with 18% thickness at root and 14% at tip. The model was driven in angle of attack oscillations about the quarter chord point. The frequency, mean and amplitude of oscillations could be pre-set. Mountings were on the floating frame of a 3-component force balance which carried the model and a variable speed motor system. Balancing masses were incorporated to avoid intereference in data aquisition. The lift and drag loadcells, the tunnel micrometer and AOA petentiometer were scanned at 70 readings per channel over a 21 second run giving 1500 datapoints in each channel. Analogue signals were conditioned by a 30 Hz low pass filter, in an attempt to remove mains noise and balance vibration effects. The data was corrected for balance interections and calibrations and wind tunnel corrections were than applied for solid and wake blockage and tunnel constraints. The accuracy of lift measured was of the order of 0.006 of lift coefficient. The rig could simulate the periodic motion experienced

by spanwise sections on a rolling wing. The schematic of data aquisition is illustrated in Fig. 6.

Simulated Icing

The parameters that determine the glaze -ice profile achieved in steady flight are many. Apart from the prevailing at mospheric conditions, the liquid water content, the icing duration, the angle of attack and he airspeed influence the flow field which in turn effect the water droplet trajectories. A typical generic glaze ice shape used was deduced from one previously used[4] in NACA 0012 aerofoil tests. Fig. 7.

STATIC AND DYNAMIC TESTS

Static tests were performed on a wing section clean configuration and with ice, to obtain the baseline data for comparison with both the real aircraft and the dynamic tests. Tests were conducted with and without forced boundary layer transition between 10% and 13% chord. The effect of roughening the ice strip was found to be significant. Hence subsequent tests employed both the rough ice strip, and the transition strip. Comparisons were approximate as the tests were run at a chord Reynolds number of 1.2×10^6, which is about one sixth that of actual aircraft. Two different aerofoil sections were involved. In particular, the real wing immediately prior to the roll upset was at a lift coefficient of 1.31. with 15° flap whole the two dimensional test wing could only achieve 1.17 with 20° flap. Results depicted in Fig. 8.

Dynamic tests simulated the accident aircraft conditions. The accident roll rate of 1 rad/s at a reduced frequency of Π. fc/U of 0.016, was used to establish the range of angle of attack and the freuency of pitching oscillations. The roll induced angle of attack variation was upto $\pm 10°$. Reduced frequencies upto 0.04 were investigated.

Intial dynamic tests disclosed, contrary to expectations, a dynamic effect on the lift even for the clean wing. Fig (8). Subsequent to

this, extensive dynamic tests were conducted concentrated around the accident values of parameters. A section of results are illustrated in Fig. (9). Note that in all cases, hysteresis is evident at stall but it is exaserbated by icing. At lower reduced frequences, the extent of hysteresis loops is reduced, but at high reduced frequences the increase is less apparent. It may further be noted that at a particular high incidence, the lift generated is dependent to a greater extent on the sign of change of angle of angle of attack than its absolute value. This perhaps supports the original hysteresis contention. Lower values of lift curve slopes compared to clean wing were also evident.

The premature stall of glaze iced wing, in conjunction with the filght test results explains the absence of stall warning. Effects of ice on roll damping were tested. Fig. (10). Wing roll damping characterestics in terms of $dC_l/d\alpha$. C_D and local rolling moment derivative indicated possibilities of negetive damping in the stall region. However, for lower incidences, icing did not indicate any adverse effects on roll stability. Further investigations, of stall loops at reduced frequences upto 0.04 were performed, at a mean incidence of 22° with + or - 9° deflection. Fig. (11). The structure of loops remained identical irrespective of the reduced frequency. However, a slight widening of the loops with increasing reduced frequency is evident. This is possible evidence to the involvement of unsteady loads and a dynamic delay in flow separation. The dynamic delay is more apparent in the iced wing. Influence of direction of change in AOA is established by the dynamic deviations from the static stalling characterestics. Note that though the deviations are propotionate, it is agravated by icing.

FLOW VISUALISATION

Flow visualisation tests were performed with surface mounted tufts and video recording. The tests were run at a Reynolds number of 0.9×10^6

Static tests on the clean wing indicated a trailing edge separation which moved forward gradually to reach mid chord at $\alpha = 12°$ and the

leading edge at α =16°. For the dynamic case, when the clean wing was oscillated at a reduced frequency of 0.0022, the mid chord separation point was reached somewhat earlier at α=7°.

Visual observations with the icing strip was distinct. A leading edge bubble separation initiated at α =5° is indicated. With increasing angle of attack, the bubble lenghtened while the trailing edged separation moved forward. At α = 13°, a rapid merging of the two separations was observed apparently indicating bubble bursting. For the dynamic test, slight discrepancies in the mid chord separation & reattachment angles of attack were observed.Further, for incidences beyond the static stall range, a quasi-steady periodic switching between separated and attached flow is exhibited at leading edge. This unsteadiness is perhaps asociated with the shedding of vortical structures from leading edge.

CONCLUSIONS

The tests performed, though highlighted the accident aircraft contitions, were only a crude simulation. Hypothetical effects of ice on roll damping stated, did not account for the roll/sideslip and roll/yaw derivatives. With wind tunnel tests, the difference in wing sections and Reynolds number were strong constraints. However, the tests did establish that the presence of leading edge glaze ice can initiate leading edge separation and reattachment causing premature stall. For a rolling wing the effect transforms into hysteresis at high incidences, and subsequently into stall loops in the stalling region. Significant influences of dynamic stall effects of ice on wing roll damping was revealed, and confirmed with roughstrip theory estimates. Thus both the hysteresis model and the stalled wing model emphasises the possible validity of a conclusion that glaze icing can cause major degradations in roll stability. The model also recomend the design philosophy of stall warning systems to incorporate the effects of glaze icing.

Further investigations on the aerodynamic effects of ice on airfraft stability and control is recommonded.

REFERENCES

1. Mckinley R.C, et. al. Aircraft Accident Report No. EW/C947. Accidents Investigations Branch (Department of Transport, U.K.) March 1987.

2. Tease. K, Waterson. J, An investigation into the lateral stability of a SHORTS SD 360, Dept. of Aeronatical Engg., The Queens University of Belfast, 1989.

3. Nair G.G An experimental investigation into the effects of Glaze icing on wing aerodynamics and lateral stability of a Shorts SD3-60. MSc Thesis, Dept.of Aero Engg.,The Queen's University of Belfast, 1992.

4. K.D.Korkan, E.J.Cross & C.C.Cromwell. Experimental Aerodynamic Charecterestics of NACA 0012 aerofoil with simulated ice. Journal of Aircraft, Vol.22.

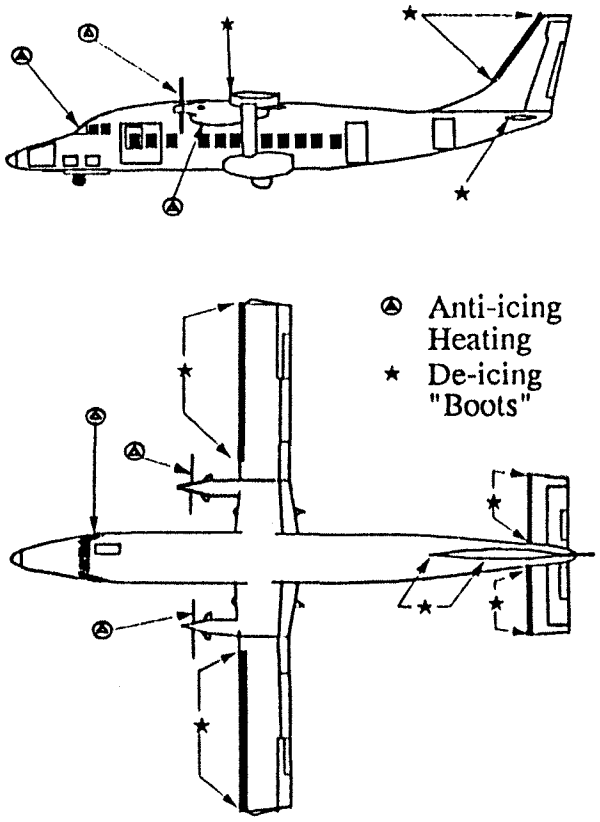

Fig. 1. SHORTS SD3-60

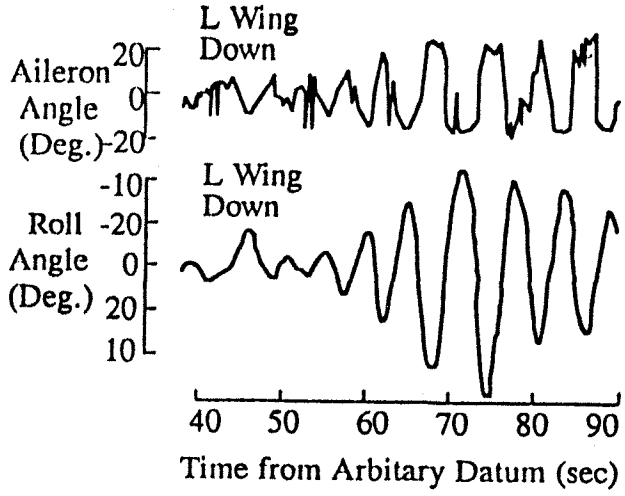

Fig. 2. FLIGHT DATA - ACCIDENT FLIGHT

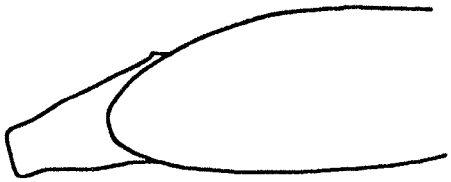

(a) Rime Ice

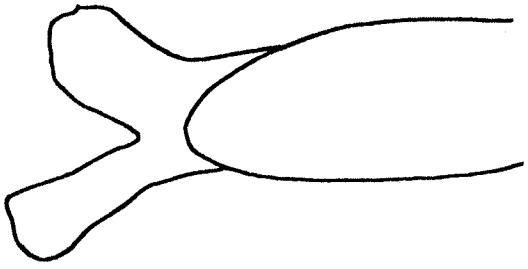

(b) Glaze Ice

Fig. 3 TYPICAL AEROFOIL ICE ACCRETIONS

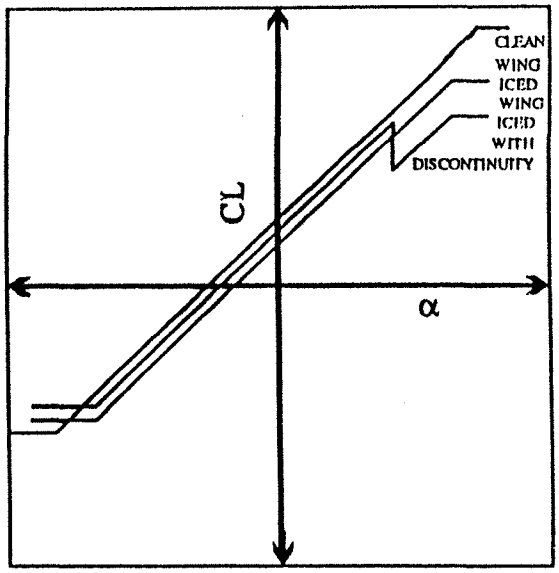

FIG. 4. MODEL LIFT CURVE

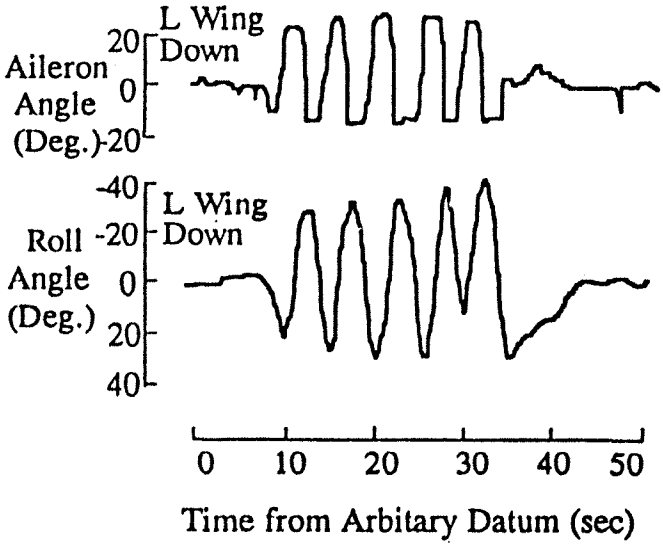

Fig. 5. FLIGHT DATA - TEST FLIGHT

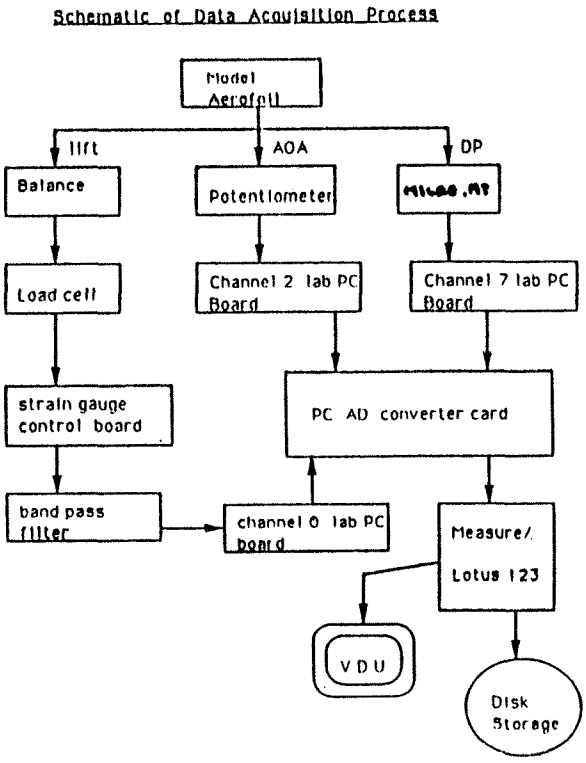

Fig. 6

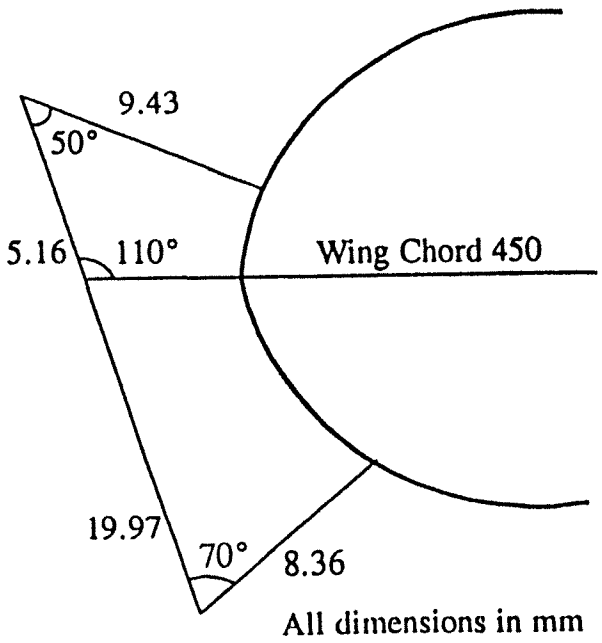

Fig. 7. GENERIC ICE PROFILE

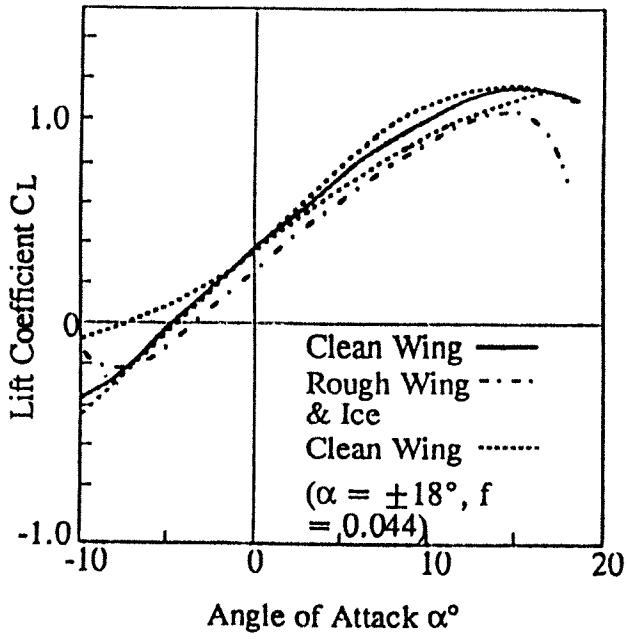

Fig. 8. COMPARISON BETWEEN SOME STATIC AND A DYNAMIC TEST, CL ~ α

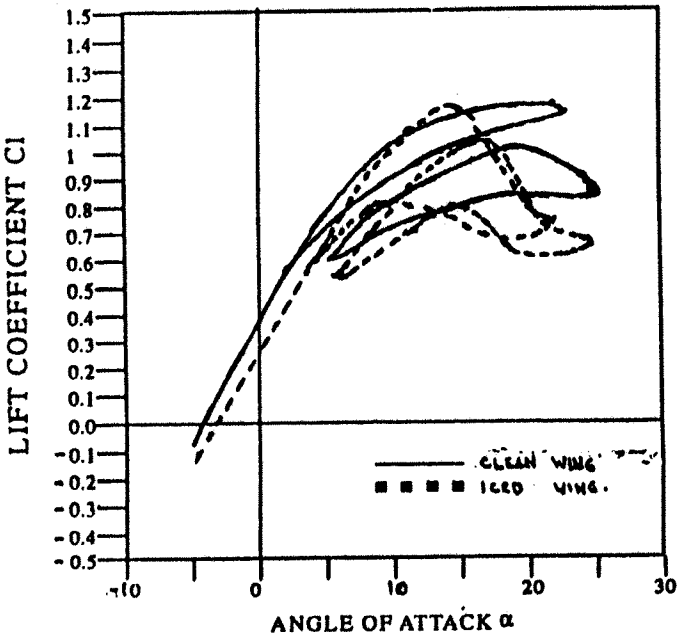

FIG. 9 DYNAMIC TESTS

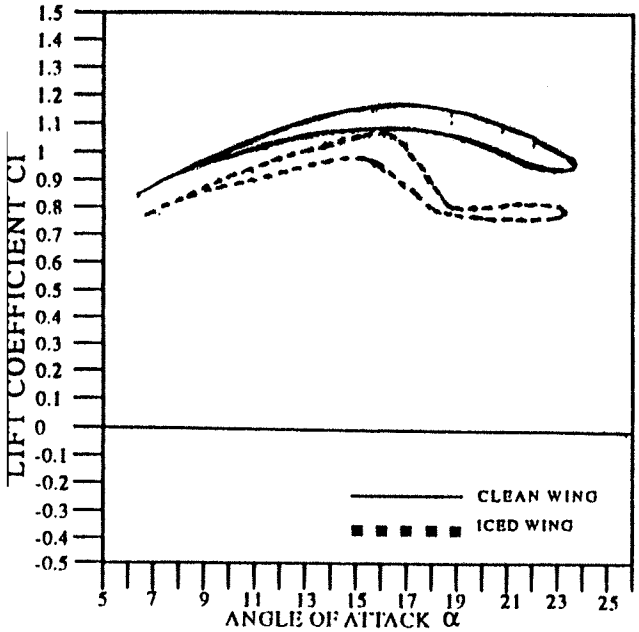

FIG. 10 ROLL SIMULATION TEST
α = 16 ± 10°

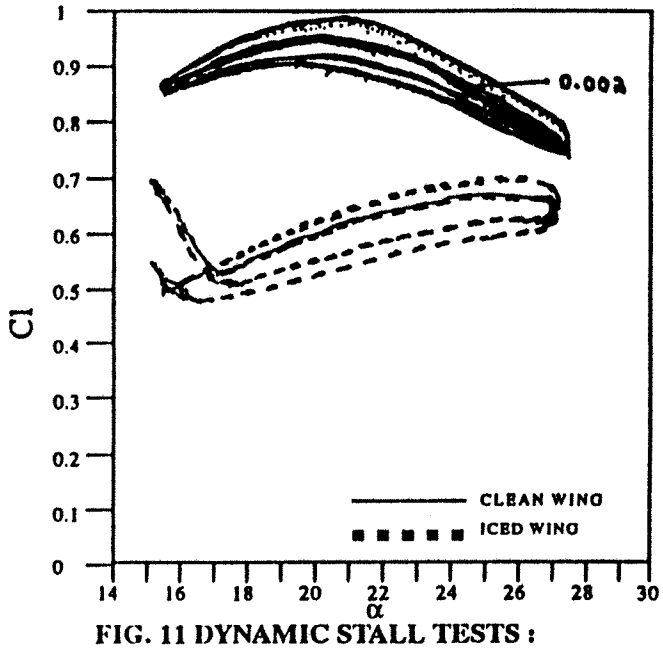

FIG. 11 DYNAMIC STALL TESTS :
Reduced Frequency 0.002 & 0.04
α = 22° ± 8°